Volume 1 | Number 1 | Jan 2013 | Pages 1–100

Dalton Transactions

An international journal of inorganic chemistry
www.rsc.org/dalton

ROYAL SOCIETY OF CHEMISTRY

ROYAL SOCIETY OF CHEMISTRY

www.rsc.org/dalton

Journal Name

ARTICLE

Mechanistic Insights on the Full Hydrogenation of 2,6-substituted Pyridine Catalyzed by the Lewis Acid $C_6F_5(CH_2)_2B(C_6F_5)_2$

Jiyang Zhao[a,b], Guoqiang Wang[a] and Shuhua Li[*,a]

The reaction mechanism for the full hydrogenation of 2-phenyl-6-methyl-pyridine catalyzed by the Lewis acid $C_6F_5(CH_2)_2B(C_6F_5)_2$ was investigated in detail by density functional theory calculations. Our calculations show that a plausible reaction pathway of the hydrogenation of pyridine contains five stages: (1) The generation of a new borane $C_6F_5(CH_2)_2B(C_6F_5)_2$ from the hydroboration of the alkene, which forms a frustrated Lewis pair (FLP) with a pyridine; (2) The activation of H_2 by FLP to yield an ion pair intermediate; (3) Intramolecular hydride transfer from the boron atom to the pyridinium cation in the ion pair intermediate to produce the 1,4-dihydropyridine; (4) Hydrogenation of the 1,4-dihydropyridine by the FLP to form the 1,4,5,6-tetrahydropyridine; (5) Hydrogenation of the 1,4,5,6-tetrahydropyridine by the FLP to yield the final piperidine. The last two hydrogenation processes follow the similar pathway, which include four steps: (a) Proton transfer from the pyridinium moiety to the substrate; (b) Dissociation of the newly generated pyridine; (c) Hydride migration from the hydridoborate moiety to the protonated substrate to produce the hydrogenated product; (d) Release of the hydrogenated product to regenerate the free borane. The full hydrogenation of pyridine is calculated to be exothermic by 16.9 kcal/mol, relative to the starting reactants. The rate-limiting step is the proton transfer in the second hydrogenation step, with a free energy barrier of 28.2 kcal/mol in gas phase (27.9 kcal/mol in toluene) at room temperature and 1.0 atm. Our results can account for the observed experimental facts.

Introduction

Homogeneous hydrogenation of unsaturated substrates is a subject of great importance in the chemical and process industries.[1] The powerful methodology in this area is the transition metal-catalyzed direct or transfer hydrogenations.[2,3] However, these transition metals are always precious and toxic. Many efforts have been made to explore non-transition-metal homogeneous catalytic hydrogenation.[4] A great breakthrough occurred in 2006 when Stephan and co-workers uncovered frustrated Lewis pairs (FLPs),[5] which can activate the heterolytic cleavage of dihydrogen under mild conditions[6] and serve as metal-free catalysts for homogeneous hydrogenation of a polar double bonds in imines, enamines, ketones, and so on.[7] A typical catalytic cycle involving FLPs[8] includes: (a) The formation of an "encounter complex" by a Lewis acid and a Lewis base; (b) Heterolytic cleavage of H_2 by FLP; (c) Hydride transfer from the center of the Lewis acid to the carbonium ion to yield the saturated product. Obviously, the mechanism of the FLP-catalyzed hydrogenation reactions is quite different from the transition metal-catalyzed hydrogenation reactions, in which substrates are activated via coordination to transition metals.[3] Furthermore, T. Repo[9] and J. Paradies[10] reported that FLPs can be used to catalyze the hydrogenation of alkynes or

olefins, although only partial catalytic reduction of substrates was achieved.

Despite these advances, full hydrogenation of heteroaromatic compounds is still a challenge for both transition metal compounds and FLPs.[11] The main reason is due to the fact that these compounds have stable aromatic structures. Recently, an important advance has been made by several groups.[12-14] They reduced pyridines completely to produce piperidine or piperidinium salts. H. F. Du and coworkers described the hydrogenation of pyridines under H_2 (50 bar) using catalytic amounts of borane catalysts generated in situ from alkenes and $HB(C_6F_5)_2$ at 100 ℃, furnishing piperidines in high yields with excellent cis stereoselectivities. D. W. Stephan and co-workers reported the successful hydrogenation of pyridines to give piperidinium salts, when the Lewis acid is $B(C_6F_5)_3$.

It is worth mentioning that the molecular mechanism of the complete hydrogenation of pyridines catalyzed by FLPs has not been established. A thorough understanding of the mechanistic details of FLP-catalyzed hydrogenation of pyridines is significant for designing more effective FLPs for hydrogenation of other heteroaromatic compounds. In this work, we have performed density functional theory (DFT) calculations to investigate the molecular mechanism for the Lewis acid-catalyzed hydrogenation of 2-phenyl-6-methyl-pyridine (as shown in Scheme 1). The Lewis acid we choose is

$C_6F_5(CH_2)_2B(C_6F_5)_2$. 2-phenyl-6-methyl-pyridine can be considered as a typical example of substituted pyridines.
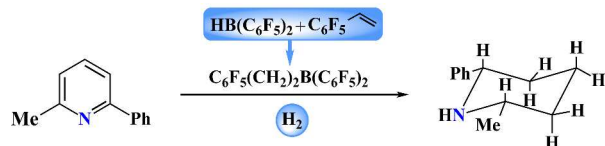
Scheme 1 Catalytic pyridine hydrogenation by the Lewis acid $C_6F_5(CH_2)_2B(C_6F_5)_2$

Computational details

Geometry optimizations of all stationary points for the studied reaction were performed with the M06-2X functional,[15] which has been proven to describe the dispersion effects very well. The 6-311G(d,p) basis set[16] was used for all atoms in substrates and the catalyst. Vibrational frequencies were obtained for all stationary points on the potential energy surface to make sure whether the optimized geometry corresponds to a minimum or a transition state. The calculated Gibbs free energies refer to T=298K and 1atm. For species in the rate-limiting step, we also calculated their Gibbs free energies at T=373K and 50 atm in toluene, which correspond to the experimental conditions. IRC calculations are performed to verify whether the transition states are truly connected by the reactants and the products. The polarization effect of the solvent (toluene) was treated with the polarizable continuum model (PCM) for species in the studied reaction. All calculations were carried out with the Gaussian 09 software package.[17]

Activation free energy barriers used in this text are defined as the free energy difference between the transition state and the most stable species (initial reactants and intermediates) in the reaction channel.

Results and discussion

In this section, we discuss the generation of the actual catalyst first. Then the successive hydrogenation of pyridine ring will be explored.

Generation of the New Borane

For this reaction, optimized geometries of all stationary points along the reaction pathway are displayed in Figure 1. The Gibbs free energy profile in gas phase is presented in Figure 2.

Our calculations show that the first step of the reaction process is the hydroboration of the alkene **2** to produce the new borane **4**. First, the B-H bond in the borane **1** attacks on the C-C double bond of **2** to form a precursor complex **3**. Then, the hydrogen atom and the boron atom add on the same face of the double bond in a concerted process via a four-membered transition state (**TS₃/₄**) to give a new borane **4**, $C_6F_5(CH_2)_2B(C_6F_5)_2$. The reaction is strongly exothermic and the barrier is only 8.8 kcal/mol (8.7 kcal/mol in toluene). This indicates that the hydroboration of alkenes is a feasible way to yield more novel boranes. Our calculations show that the acidity of the product **4** is stronger than that of **1**.

The Activation of H₂ by the Frustrated Lewis Pair

For this step, optimized geometries of all stationary points along the reaction pathway are displayed in Figure 3. The Gibbs free energy profile in gas phase is presented in Figure 4.
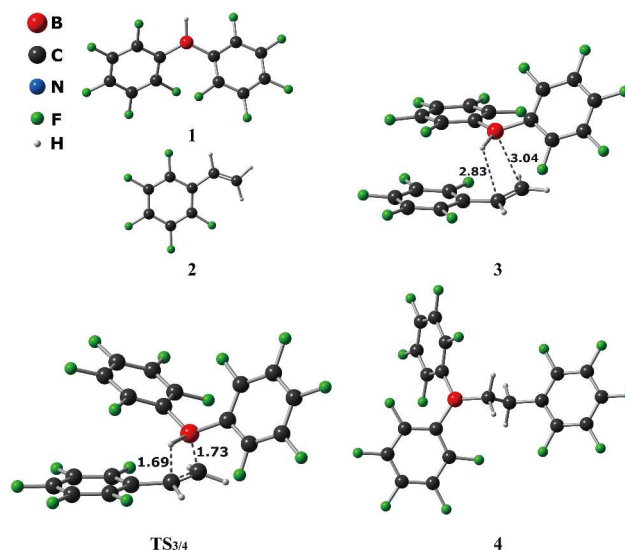

Fig. 1 Optimized structures of some species involved in the generation of the new borane **4**. Selected bond distances are given in Å.
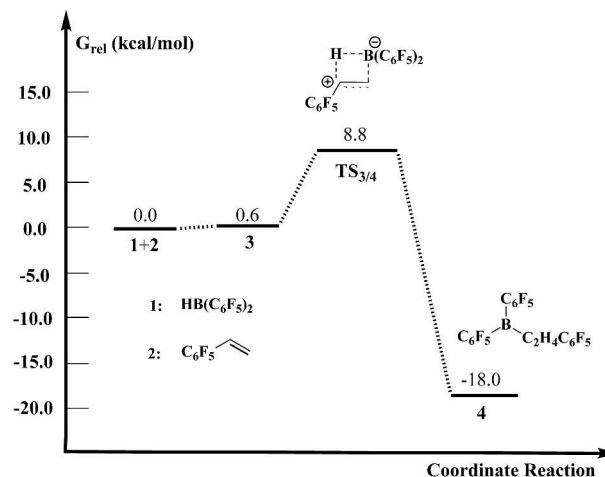

Fig. 2 Gibbs free energy profile for the generation of the new borane **4**. Free energies are calculated at 298.15 K and 1.0 atm in the gas phase.

The interaction between the pyridine **5** and the borane **4** may lead to two possible isomers. One is the FLP **6**. Another is the classical Lewis adduct **6a** with the B-N distance of 1.70 Å. **6a** lies 1.6 kcal/mol in free energy below **6**, suggesting that an equilibrium between **6a** and **6** may exist.[18] However, **6** is the reactive intermediate for subsequent reactions as it can facilitate the activation of H₂, as demonstrated below. It is expected that **6a** can easily transform into **6** via rearrangement of Lewis acid and Lewis base in solutions.

The activation of H₂ by the FLP **6** occurs in a stepwise manner.[19] First, H₂ coordinates to the boron center of species **6** to form the species **7**, which is then deprotonated by the nitrogen atom of the pyridine ring to yield a pyridinium hydridoborate ion pair **8**. In the species **7**, the two B-H distances are 1.64 Å and 1.75 Å, respectively. The H-H bond is

elongated to 0.77 Å, showing that the H–H bond is activated. There is also a non-covalent interaction between the nitrogen atom of the pyridine ring and a nearby hydrogen atom of H_2 (the N-H distance is 2.17 Å). The subsequent H_2 cleavage process occurs via the transition state $TS_{7/8}$, which lies 19.0 kcal/mol (19.4 kcal/mol in toluene) in free energy above the most stable intermediate **6a** and H_2. In $TS_{7/8}$, the H-H bond is elongated to 0.87 Å, and the B-H and N-H distances are 1.39 Å and 1.54 Å, respectively. The formation of the ion pair **8** is found to be exothermic by 15.3 kcal/mol (relative to the starting reactants), because this intermediate is stabilized by N-H$^+\cdots^-$H-B (2.35 Å) and N-H$\cdots$F-C (1.98 Å) non-covalent contacts. Species **8** is the key intermediate for subsequent hydrogenation steps.

For the ion pair **8**, we also located some of its other conformers, in which the relative position of the pyridium ion and the borohydride ion is different. They all have slightly higher energies, whose relative energies (relative to species **8**) are within 4 kcal/mol. For two isomers, which are above species **8** in free energy by 0.5 and 3.2 kcal/mol, respectively, we have explored their possible role in the following hydrogenation reaction. Our calculations show that the reaction mechanism and the rate-limiting step with these two isomers as the key intermediate are the same as those with species **8** as the key intermediate. For brevity, only the results with species **8** as the key intermediate in the hydrogenation reaction are discussed in the subsections below.
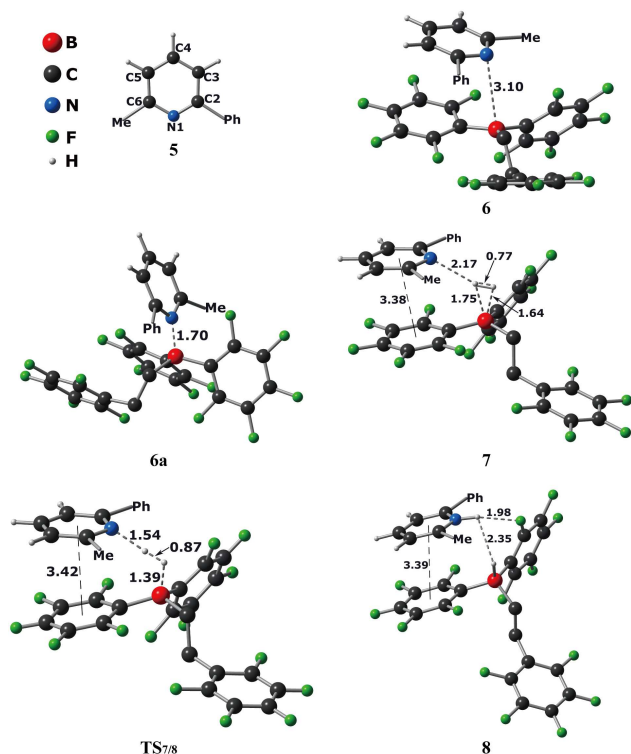

Fig. 3 Optimized structures of some species involved in H_2 cleavage step. Selected bond distances are given in Å. The hydrogen atoms of the species are omitted for clarity.
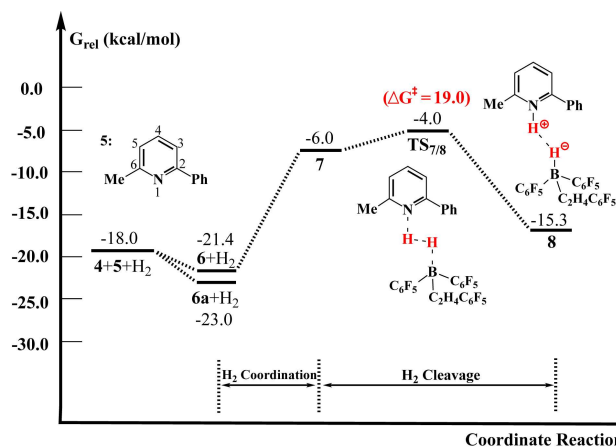

Fig. 4 Gibbs free energy profile for the H_2 cleavage step. Relative free energies calculated at 298.15 K and 1.0 atm in the gas phase (with respect to that of the reactants) are given. The free energy barrier $\Delta G^{\neq}$ is relative to that of the most stable intermediate **6a** and H_2.

First Hydrogenation Step

For this step, optimized geometries of all stationary points along the reaction pathway are displayed in Figure 5. The Gibbs free energy profile in gas phase is presented in Figure 6. First, the ion pair **8** is likely to transform into another isomer **9** by intramolecular rearrangement. In the intermediate **9**, the B-H bond is oriented towards the center of the pyridinium cation. In the next step, the hydride transfer from the B atom to the C4 atom of the pyridinium cation occurs through the transition state $TS_{9/10}$ to form the intermediate **10**, in which 1,4-dihydropyridine **11** and the borane **4** are loosely bound. In $TS_{9/10}$, the B-H and C-H distances are 1.31 and 1.58 Å, respectively. The corresponding free energy barrier of this hydride transfer process is 24.0 kcal/mol (relative to the most stable intermediate **6a**). Then, the product **10** will dissociate to generate the 1,4-dihydropyridine **11** (the product of the first hydrogenation of the pyridine **5**) and the borane **4**. Interestingly, the 1,4-dihydropyridine **11** has a nearly planar structure. The first hydrogenation step of the pyridine **5** is endothermic by 12.8 kcal/mol, relative to the starting reactants (**5** and H_2). The rate-limiting step is the hydride transfer process with a free energy barrier of 24.0 kcal/mol (23.2 kcal/mol in toluene), as mentioned earlier. Moreover, the product **4** and the pyridine **5**, will continue to form an FLP, which then activates H_2 to yield the key intermediate **8**.

In the meantime, we also explore the possibility of a hydride transfer from the B atom to the C2 or C6 atom in the pyridinium cation, which could generate 1,2-dihydropyridine or 1,6-dihydropyridine. The corresponding reaction barriers are calculated to be 25.1 and 20.8 kcal/mol (relative to the most stable intermediate **6a**), respectively. However, our calculations show that the further hydrogenation of 1,2-dihydropyridine or 1,6-dihydropyridine in the following steps involves significantly higher energy barriers. Hence, we will not discuss the reaction pathways for the formation of 1,2-dihydropyridine or 1,6-dihydropyridine.
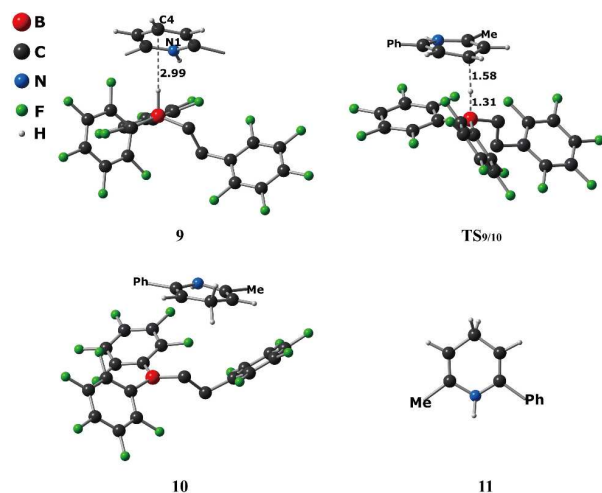
Fig. 5 Optimized structures of some species involved in the first hydrogenation step. Selected bond distances are given in Å. The hydrogen atoms of the species are omitted for clarity.
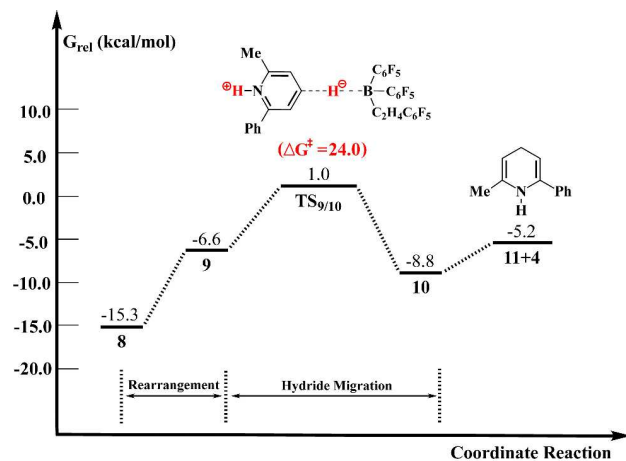

Fig. 6 Gibbs free energy profile for the first hydrogenation step. Relative free energies calculated at 298.15 K and 1.0 atm in the gas phase (with respect to that of the reactants) are given. The free energy barrier $\Delta G^{\neq}$ is relative to that of the most stable intermediate **6a** and H_2.

Second Hydrogenation Step

There are two double bonds (C2=C3 and C5=C6) in the 1,4-dihydropyridine **11**. Since the hydrogenation of the C5=C6 double bond facilitates the conjugation between pyridine and the lateral phenyl substituent, we expect that the hydrogenation of the C5=C6 double bond may occur at the second hydrogenation step. For this reaction step, the optimized structures of all stationary points along the reaction pathway are displayed in Figure 7. The Gibbs free energy profile in gas phase is presented in Figure 8.

First, the 1,4-dihydropyridine **11** approaches the key intermediate **8** to afford a stable complex **12**, which is stabilized by N-H⋯N hydrogen-bond (2.26 Å) and π - π stacking (3.36 Å) interactions. Then, the nitrogen-bound proton transfers from the pyridinium cation to the C5 atom of the 1,4-dihydropyridine moiety to produce the intermediate **13**, through the transition state **TS₁₂/₁₃**. This proton transfer step is endothermic by 3.2

kcal/mol, with a free energy barrier of 28.2 kcal/mol (relative to the most stable intermediate **6a**). After a loosely bound pyridine is released, species **13** will convert into the ion pair complex **14**, in which the pyridinium and the hydridoborate forms an ion pair. In the next step, the hydride may migrate from the boron atom to the C6 atom of the 1,4-dihydropyridinium ion through the transition state **TS₁₄/₁₅** to give the intermediate **15**. The corresponding free energy barrier of this hydride transfer process is 24.0 kcal/mol (relative to the most stable intermediate **6a**). Then, the intermediate **15** will dissociate to give the 1,4,5,6-tetrahydropyridine **16** and the borane **4**. Finally, the 1,4,5,6-tetrahydropyridine **16** can isomerize via the transition state **TS₁₆/₁₇** to produce the thermodynamically more stable isomer **17**, which is the product of the second hydrogenation of the pyridine **5**. This isomerization process has a relatively low free energy barrier of 9.7 kcal/mol (relative to the most stable intermediate **6a**).

The second hydrogenation step of the pyridine **5** is exothermic by 2.4 kcal/mol (relative to the starting reactants, **5** and H_2). The rate-limiting step is the proton transfer process with a free energy barrier of 28.2 kcal/mol, as described above. When the solvent (toluene) effect is considered, the free energy barrier of the proton transfer step decreases slightly to 27.9 kcal/mol. It is obvious that this hydrogenation process is more difficult than the first hydrogenation step.
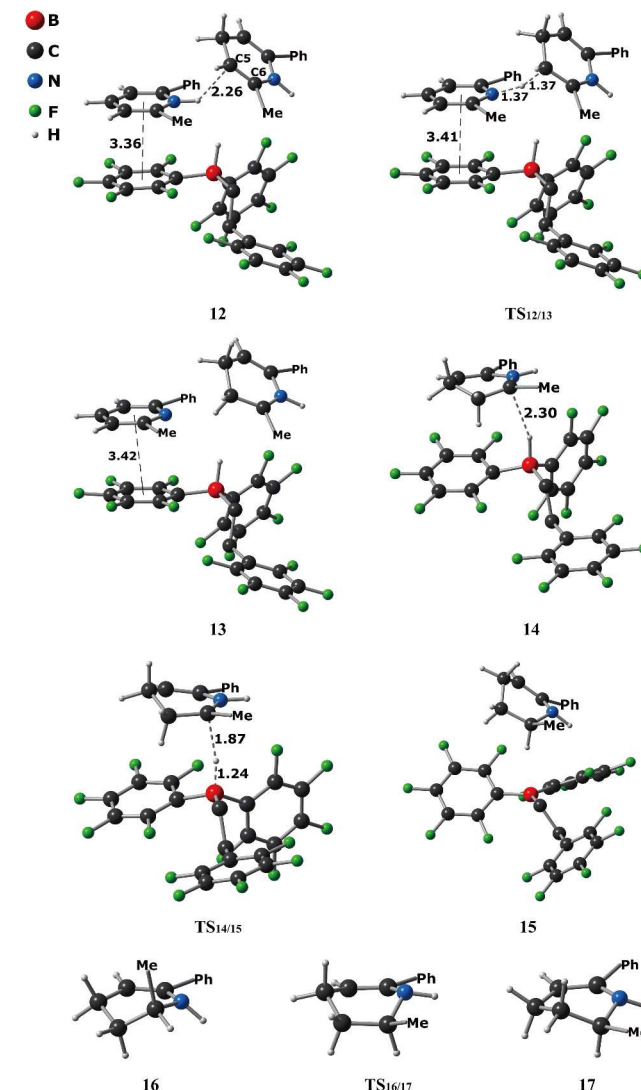
Fig. 7 Optimized geometries of some species involved in the second hydrogenation step. Selected bond distances are given in Å. The hydrogen atoms of the species are omitted for clarity.

It is interesting to understand why the pyridine **5** could be hydrogenated successively by the ion pair **8**, because the aromatic ring is usually difficult to be hydrogenated. To get some insight into the factors that contribute to the hydrogenation of the pyridine, we have calculated the proton and hydride affinities[20] of the reactants and the FLP components. The calculated results are shown in Scheme 2.

The calculated proton affinity of **11** is 232.1 kcal/mol, which is slightly larger than that of the pyridine **5** (231.2 kcal/mol). At

the same time, the calculated hydride affinity of **[11H]**$^+$ is 199.5 kcal/mol, which is much larger than that of the borane **4** (125.8 kcal/mol). These data suggest that the unsaturated bond (C5=C6) of the reactant **11** is thermodynamically favorable in taking a proton and a hydride from the generated FLP **8**. The weak acidity of **4** plays a major role in driving the hydrogenation reaction.

In addition, if we choose the C2=C3 double bond in the 1,4-dihydropyridine **11** to be hydrogenated, the free energy barrier in the rate-limiting step will rise up to 32.1 kcal/mol. Thus, the most probable sequence of hydrogenation of the pyridine ring is N1-C4-C5-C6-C3-C2.
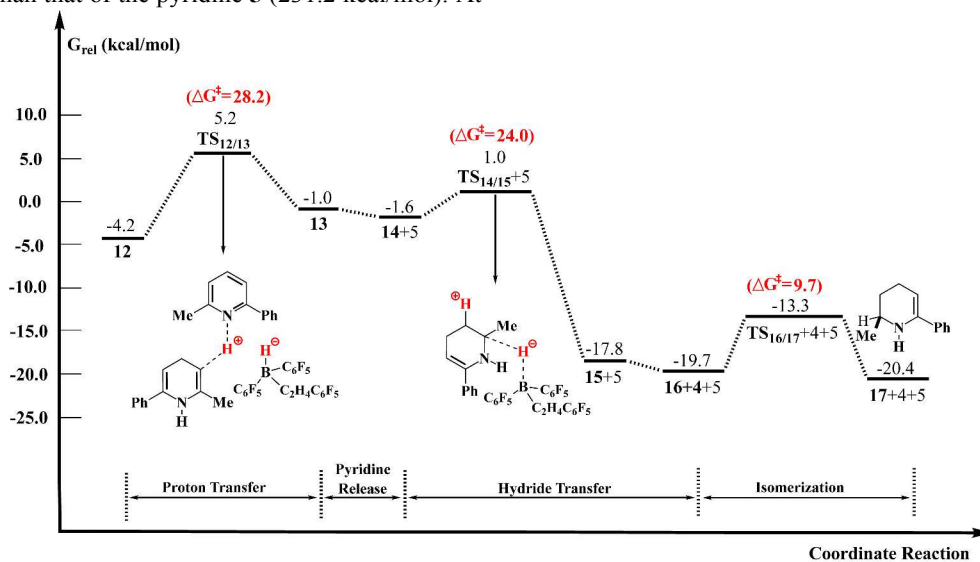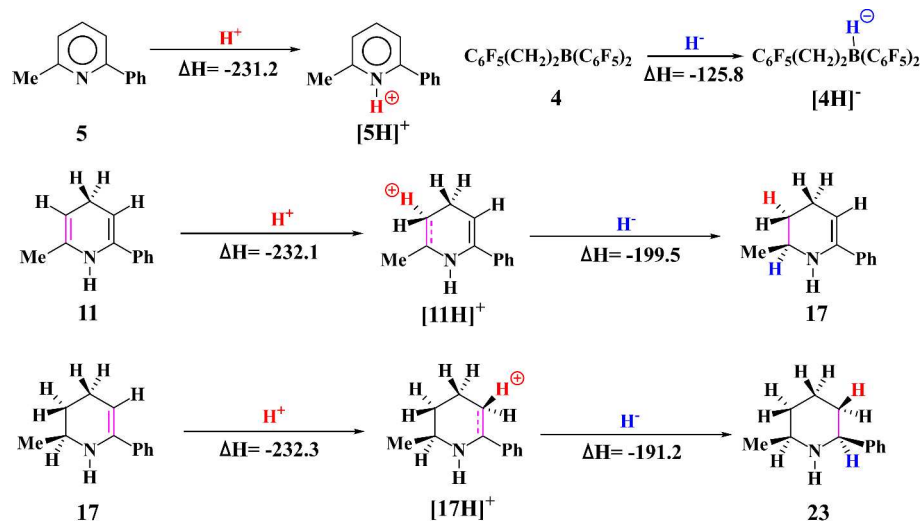

Fig. 8 Gibbs free energy profile for second hydrogenation step. Relative free energies calculated at 298.15 K and 1.0 atm in the gas phase (with respect to that of the reactants) are given. The free energy barrier $\Delta G^{\neq}$ is relative to the most stable intermediate **6a** and H$_2$.

Scheme 2 The calculated proton and hydride affinities of pyridine, borane and key intermediates in the reaction processes. All energies are given in kcal/mol.

Third Hydrogenation Step

The hydrogenation process of the unsaturated C2=C3 bond in the pyridine ring is very similar to that in the second

hydrogenation step. Optimized geometries of all stationary points along the third hydrogenation step are displayed in Figure 9. The Gibbs free energy profile in gas phase are presented in Figure 10. It can be seen from Figure 10 that the barriers of the proton transfer (via **TS$_{18/19}$**) and the hydride

transfer (via **TS$_{21/22}$**) in this step are only 15.1 and 7.3 kcal/mol (relative to the most stable intermediate **6a** and H$_2$), respectively. The barrier of the proton transfer step increases slightly to 15.2 kcal/mol, when the solvent (toluene) effect is considered. The final hydrogenation product is *cis*-piperidine **23**, with a chair-like six-membered ring. This result is consistent with the experimental observation. The third hydrogenation step is exothermic by 16.9 kcal/mol, relative to the starting reactants (**5** and H$_2$). As shown in Scheme 2, the calculated proton affinity of **17** (232.3 kcal/mol) and the hydride affinity of **[17H]$^+$** (191.2 kcal/mol) also suggest that the third hydrogenation process by the key FLP intermediate is thermodynamically feasible.

Furthermore, we also consider the direct hydrogenation of the 1,4,5,6-tetrahydropyridine **17** by the borane **4** in this step. First, the activation of H$_2$ by the borane **4** and the 1,4,5,6-tetrahydropyridine **17** proceeds through the transition state **TS$_{B-C}$**, generating the ion pair **24**. The utilization of carbon Lewis acid based FLP for H$_2$ activation has been realized by experiment.[21] Then the species **24** may isomerize into the more stable complex **21**. The subsequent hydride transfer process, which produces the final product, will be the same as described above. Since the free energy barrier of this pathway (21.2 kcal/mol) is much higher than that mentioned above, this reaction channel is unlikely for the third hydrogenation step.
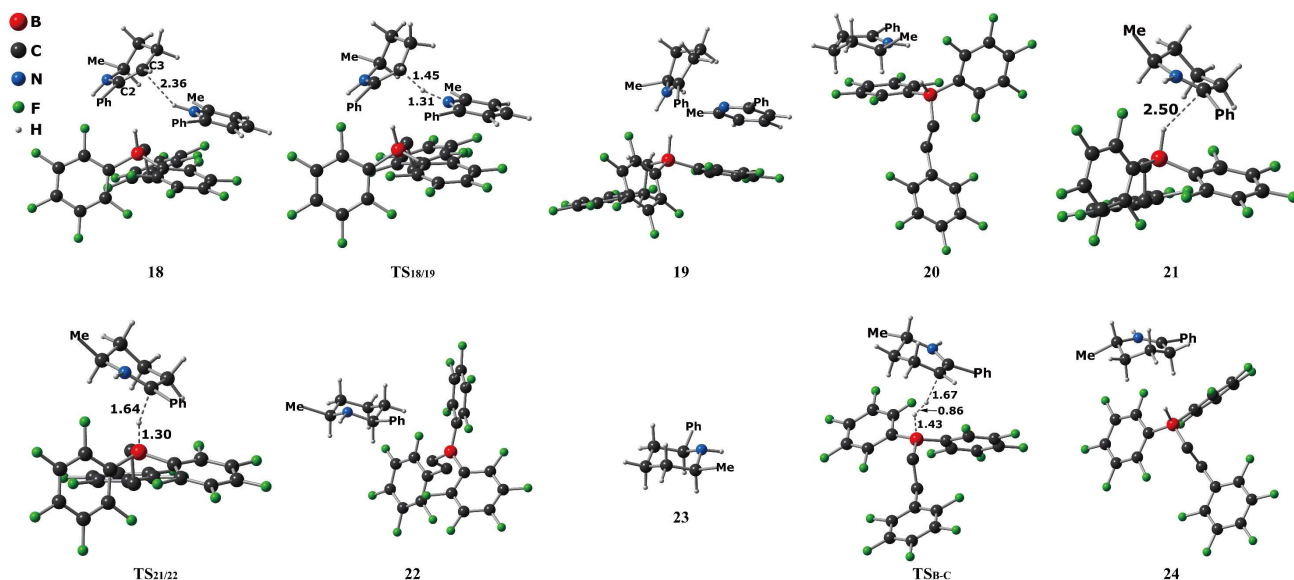

Fig. 9 Optimized geometries of some species involved in the third hydrogenation step. Selected bond distances are given in Å. The hydrogen atoms of the species are omitted for clarity.
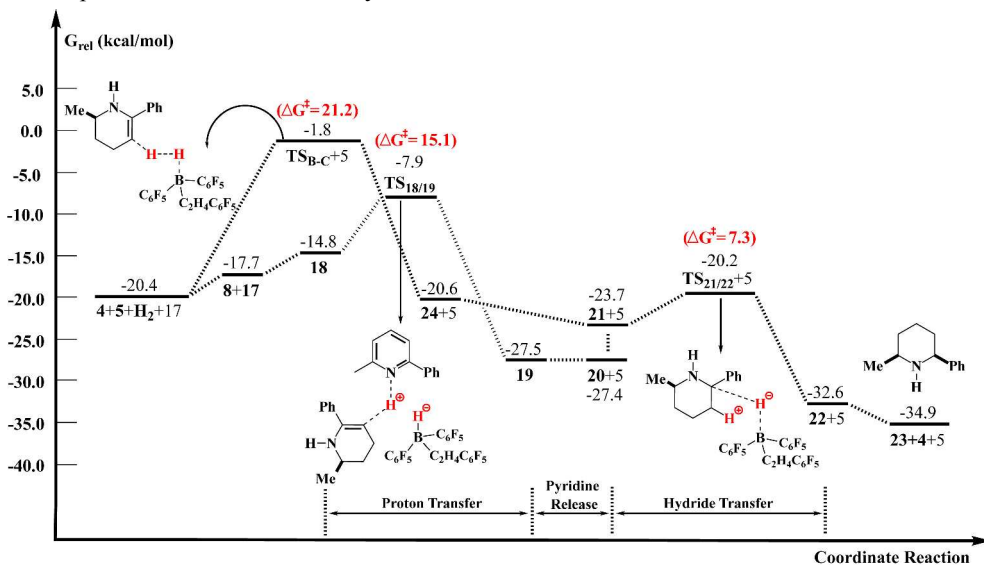

Fig. 10 Gibbs free energy profile for the third hydrogenation step. Relative free energies calculated at 298.15 K and 1.0 atm in the gas phase (with respect to that of the reactants) are given. The free energy barrier $\Delta G^{\neq}$ is relative to that of the most stable intermediate **6a** and H$_2$.

In addition, we also investigate the process of generating another product, *trans*-piperidine. The barrier of the protonation step in the third hydrogenation step is 16.4 kcal/mol, which is higher than that (15.1 kcal/mol) of the similar process in the generation of *cis*-piperidine. More importantly, the *cis*-piperidine with equatorial phenyl and methyl group is 1.9 kcal/mol lower in free energy than the *trans*-piperidine. This result is consistent with the experimental fact that the *cis*:*trans* diastereomeric ratio is 95:5.

Stephan et al[13] reported that the hydrogenation product, piperidine can continue to active H_2 to produce the corresponding piperidinium salt, if the Lewis acid $B(C_6F_5)_3$ is employed. However, in the case of the borane **4**, no piperidinium salt was observed.[12] Our calculations show that the splitting of dihydrogen by the possible FLP, **23** and **4**, is endothermic by 6.2 kcal/mol (3.2 kcal/mol in toluene), relative to the Lewis adduct (generated by **23** and **4**) and H_2. This result can be used to account for the corresponding experimental fact.

Do the partially hydrogenated substrates act as the Lewis base component of an FLP to activate H_2?

It is worthwhile to investigate whether the partially hydrogenated products **11** and **17** can act as the Lewis base partner of the Lewis acid **4** in an FLP to activate H_2. Our calculations show that the reaction barriers of the H_2 activation by the corresponding FLPs (formed by the Lewis acid **4** and the Lewis bases **11** or **17**) are 34.7 and 25.0 kcal/mol, respectively. As discussed above, the barrier of H_2 cleavage by the FLP **6** (formed by the Lewis acid **4** and the pyridine **5**) is only 19.0

kcal/mol. Thus, the possibility of the partially hydrogenated substrates acting as the Lewis base partner of the Lewis acid **4** can be excluded.

Conclusions

We have performed detailed DFT calculations to explore the molecular mechanism of the hydrogenation of pyridine to yield the piperidine, in the presence of the Lewis acid, $C_6F_5(CH_2)_2B(C_6F_5)_2$. The main conclusion drawn from our present study can be summarized as follows:

(1) The actual catalyst for the hydrogenation of pyridine is the borane **4**, generated from the hydroboration of the alkene.

(2) The borane **4** and the pyridine form a FLP. This FLP then activates H_2 to produce the pyridinium hydridoborate ion pair, which is the key intermediate for the further hydrogenation of the partially hydrogenated product. In the next step, the hydride in the hydridoborate moiety transfers from the boron atom to the C4 atom in the pyridinium moiety to produce 1,4-dihydropyridine.

(3) The subsequent second and third hydrogenation steps of the substrate (the partially hydrogenated product) occur through the similar steps: (a) Proton transfer from the pyridinium moiety to the substrate; (b) Dissociation of the newly generated pyridine; (c) Hydride migration from the hydridoborate moiety to the protonated substrate to produce the hydrogenated product; (d) Release of the hydrogenated product to regenerate the free borane.
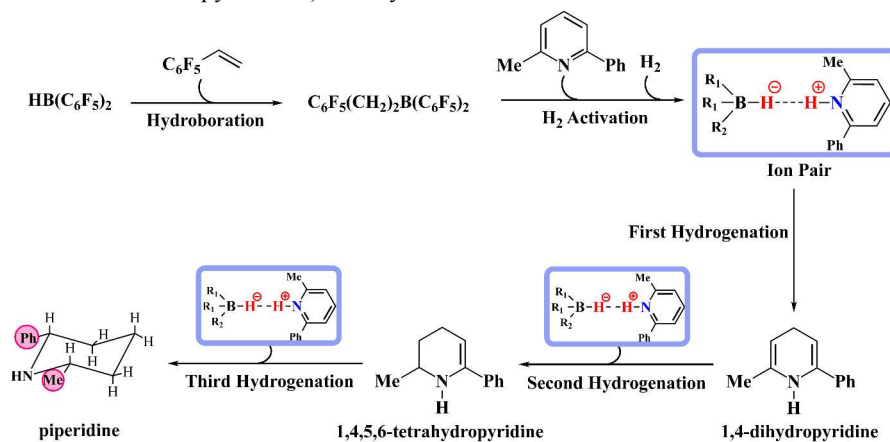
Scheme 3 The proposed pathway for the full hydrogenation of pyridine to yield the piperidine.

The proposed pathway from our study can be summarized in Scheme 3. Our calculations show that the full hydrogenation of pyridine is exothermic by 16.9 kcal/mol, relative to the starting reactants (**5** and H_2). The rate-limiting step is the proton transfer in the second hydrogenation step, with a free energy barrier of 27.9 kcal/mol in toluene at room temperature and 1.0 atm. At T=373K and 50.0 atm in toluene, the free energy barrier of this rate-limiting step decreases slightly to 27.0 kcal/mol. Our results are in good accord with the observed experimental facts. The results provide important insight into the full hydrogenation of pyridine catalyzed by the FLP, which may be useful in designing more effective FLP catalysts for hydrogenation of other heteroaromatic compounds.

Acknowledgements

Notes and references

[a] School of Chemistry and Chemical Engineering, Key Laboratory of Mesoscopic Chemistry of Ministry of Education, Institute of Theoretical and Computational Chemistry, Nanjing University, Nanjing 210093, People's Republic of China. Email: shuhua@nju.edu.cn; Fax: +86 02583686466; Tel: +86 02583686465
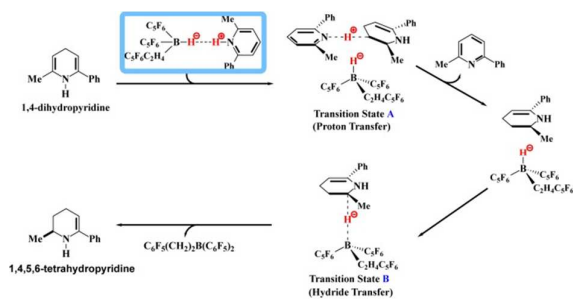
[b] Office of Science and Technology, Nanjing Xiaozhuang University, Nanjing 211171, People's Republic of China. jyzhao1981@163.com; Fax: +86 02583686466; Tel: +86 02583686465

1. (a) J. A. Osborn, F. H. Jardine, J. F. Young and G. Wilkinso, *J. Chem. Soc. A.*, 1966, **88**, 1711-1713; (b) P. S. Hallman, D. Evans, J. A. Osborn and G. Wilkinson, *Chem. Commun.*, 1967, **7**, 305-306; (c) *Acc. Chem. Res.*, 2007, **40**, special issue 12 on hydrogenation and transfer hydrogenation; (d) *Adv. Synth. Catal.*, 2003, **345**, special issue 1-2 on catalytic hydrogenation; (e) R. Yamaguchi, C. Ikeda, Y. Takahashi and K.-i Fujita, *J. Am. Chem. Soc.*, 2009, **131**, 8410-8412; (f) S. Monfette, Z. R. Turner, S. P. Semproni and P. J. Chirik, *J. Am. Chem. Soc.*, 2012, **134**, 4561-4564.

2. (a) W. J. Tang and X. M. Zhang, *Chem. Rev.*, 2003, **103**, 3029-3069; (b) A. Falrello, A. Bachelier, M. Urrutigoïty and P. Kalck, *Coord. Chem. Rev.*, 2010, **254**, 273-287; (c) Z. K. Yu, W. W. Jin and Q. B. Jiang, *Angew. Chem. Int. Ed.*, 2012, **51**, 6060-6072; (d) M. X. Chang, Y. H. Huang, S. D. Liu, Y. G. Chen, S. W. Krska, I.W. Davie and X. M. Zhang, *Angew. Chem. Int. Ed.*, 2014, **53**, 12761-12764.

3. (a) C. R. Landis, P. Hilfenhaus and S. Feldgus, *J. Am. Chem. Soc.*, 1999, **121**, 8741-8754; (b) D. A. Alonso, P. Brandt, S. J. M. Nordin and P. G. Andersson, *J. Am. Chem. Soc.*, 1999, **121**, 9580-9588; (c) Y. B. Fan, X. H. Cui, K. Burgess and M. B. Hall, *J. Am. Chem. Soc.*, 2004, **126**, 16688-16689; (d) A. Forbes, V. Verdolino, P. Helquist and O. Wiest, *Computational. Organometallic. Chemistry*. Springer-Verlag Berlin Heidelberg, 2012.

4. (a) A. Berkessel, T. J. S. Schubert, T. N. Mueller, *J. Am. Chem. Soc.*, 2002, **124**, 8693-8698; (b) Y. Peng, B. D. Ellis, X. Wang and P. P. Power, *J. Am. Chem. Soc.*, 2008, **130**, 12268-12269; (c) J. Spielmann, F. Buch and S. Harder, *Angew. Chem. Int. Ed.*, 2008, **47**, 9434-9438; *Angew. Chem.* 2008, **120**, 9576-9580; (d) G. X. Zeng and S. Li, *Inorg. Chem.*, 2010, **49**, 3361-3369; (e) S. G. Ouellet, A. M. Walji and D. W. C. MacMillan, *Acc. Chem. Res.*, 2007, **40**, 1327-1339.

5. G. C. Welch, R. R. S. Juan, J. D. Masuda and D. W. Stephan, *Science.*, 2006, **314**, 1124-1126.

6. (a) V. Sumerin, F. Schulz, M. Nieger, M. Leskelä, T. Repo and B. Rieger, *Angew. Chem. Int. Ed.*, 2008, **47**, 6001-6003; (b) V. Sumerin, F. Schulz, M. Atsumi, C. Wang, M. Nieger, M. Leskelä, T. Repo, P. Pyykkö and B. Rieger, *J. Am. Chem. Soc.*, 2008, **130**, 14117-14119; (c) S. J. Geier, T. M. Gilbert and D. W. Stephan, *J. Am. Chem. Soc.*, 2008, **130**, 12632-12633; (d) E. R. Clark, A. Del Grosso and M. J. Ingleson, *Chem.-Eur. J.*, 2013, **19**, 2462-2466; (e) Y. Guo and S. Li, *Inorg. Chem.*, 2008, **47**, 6212-6219; (f) G. Lu, P. Zhang, D. Sun, L. Wang, K. Zhou, Z.-X Wang and G.-C Guo, *Chem. Sci.*, 2014, **5**, 1082-1090; (g) X. Wang, G. Kehr, C. G. Daniliuc and G. Erker, *J. Am. Chem. Soc.*, 2014, **136**, 3293–3303; (h) S. J. K. Forrest, J. Clifton, N. Fey, P. G. Pringle, H. A. Sparkes and D. F. Wass, *Angew. Chem. Int. Ed.*, 2015, **54**, 2223-2227.

7. (a) D. W. Stephan, *Org. Biomol. Chem.*, 2012, **10**, 5740-5746; (b) P. A. Chase, T. Jurca and D. W. Stephan, *Chem.Commun.*, 2008, 1701-1703; (c) C. M. Mömming, S. Frömel, G. Kehr, R. Fröhlich, S. Grimme and G. Erker, *J. Am. Chem. Soc.*, 2009, **131**, 12280-12289; (d) H. Wang, R. Frohlich, G. Kehr and G. Erker, *Chem.Commun.*,

2008, 5966-5968; (e) D. T. Hog and M. Oestreich, *Eur. J. Org. Chem.*, 2009, 5047-5056; (f) J. M. Farrell, J. A. Hatnean and D. W. Stephan, *J. Am. Chem. Soc.*, 2012, **134**, 15728-15731; (g) T. Mahdi, Z. M. Heiden, S. Grimme and D. W. Stephan, *J. Am. Chem. Soc.*, 2012, **134**, 4088-4091; (h) J. Paradies, *Angew. Chem. Int. Ed.*, 2014, **53**, 3552-3557; (i) Z, Zhang and H, Du, *Angew. Chem. Int. Ed.*, 2015, **54**, 623-626; (j) G, LI, Y, Liu and H, Du, *Org. Biomol. Chem.*, 2015, **13**, 2875-2878; (k) D. W. Stephan, *Acc. Chem. Res.*, 2015, **48**, 306–316.

8. (a) T. A. Rokob, A. Hamza, A. Stirling and I. Pápai, *J. Am. Chem. Soc.*, 2009, **131**, 2029-2036; (b) T. Privalov, *Dalton. Trans.*, 2009, 2229-2237; (c) J. Nyhlen and T. Privalov, *Dalton. Trans.*, 2009, 5780-5786; (d) S. Bhunya and A. Paul, *Chem. Eur. J.*, 2013, **19**, 11541-11546.

9. K. Chernichenko, Á. Madarász, I. Pápai, M. Nieger, M. Leskelä and T. Repo, *Nat. Chem.*, 2013, **5**, 718-723.

10. L. Greb, P. Oña-Burgos, B. Schirmer, S. Grimme, D. W. Stephan and J. Paradies, *Angew. Chem. Int. Ed.*, 2012, **51**, 10164-10168.

11. (a) C. Y. Legault and A. B. Charette, *J. Am. Chem. Soc.*, 2005, **127**, 8966-8967; (b) Z. S. Ye, M. W. Chen, Q. A. Chen, L. Shi, Y. Duan and Y. G. Zhou, *Angew. Chem. Int. Ed.*, 2012, **51**, 10181-10184; (c) S. J. Geier, P. A. Chase and D. W. Stephan, *Chem.Commun.*, 2010, **46**, 4884-4886; (d) Y. Segawa and D. W. Stephan, *Chem.Commun.*, 2012, **48**, 11963-11965; (e) G. Erős, K. Nagy, H. Mehdi, I. Pápai, P. Nagy, P. Király, G. Tárkányi and T. Soós, *Chem.-Eur. J.*, 2012, **18**, 574-585; (f) L. Perrin, E. L. Werkema, O. Eisenstein and R. A. Andersen, *Inorg. Chem.*, 2014, **53**, 6361-6373.

12. Y. Liu and H. Du, *J. Am. Chem. Soc.*, 2013, **135**, 12968-12971.

13. T.Mahdi, J. N. Del Castillo and D. W. Stephan, *Organometallics*, 2013, **32**, 1971-1978.

14. P. Eisenberger, B. P. Bestvater, E. C. Keske and C. M. Crudden, *Angew. Chem. Int. Ed.*, 2015, **54**, 2467–2471.

15. (a) Y. Zhao, N. E. Schultz and D. G. Truhlar, *J. Chem. Theory Comput.*, 2006, **2**, 364-382; (b) Y. Zhao and D. G. Truhlar, *J. Chem. Phys.*, 2006, **125**, 194101-194118; (c) Y. Zhao and D. G. Truhlar, *J. Phys. Chem. A.*, 2006, **110**, 13126-13130.

16. R. Krishnan, J. S. Binkley, R. Seeger and J. A. Pople, *J. Chem. Phys.*, 1980, **72**, 650-654.

17. M. J. Frisch, et al, Gaussian 09, Revision B.01; Gaussian, Inc., Wallingford CT, 2010.

18. S. J. Geier and D. W. Stephan, *J. Am. Chem. Soc.*, 2009, **131**, 3476-3477.

19. Z. Lu, Z. Cheng, Z. Chen, L. Weng, Z. H. Li and H. Wang, *Angew. Chem. Int. Ed.*, 2011, **50**, 12227-12231.

20. (a) D. J. Grant and D. A. David, *Inorg. Chem.*, 2009, **48**, 8811-8821; (b) C.-H. Lim, A. M. Holder and J. T. Hynes and C. B. Musgrave, *Inorg. Chem.*, 2013, **52**, 10062-10066.

21. (a) E. R. Clark and M. J. Ingleson, *Angew. Chem. Int. Ed.* 2014, **53**, 11306-22309; (b) Y. Wang, W. Chen, Z. Lu, Z. H. Li and H. Wang, *Angew. Chem. Int. Ed.*, 2013, **52**, 7496-7499; (c) W. Piers, A. Y. Houghton, V. Karttunen and H. M. Tuononen, *Chem. Commun.*, 2014, **50**, 1295-1298.

Table of Contents

Computational study indicates that the pyridinium hydridoborate ion pair is the key intermediate for the full hydrogenation of 2,6-substituted pyridine catalyzed by the Lewis acid $C_6F_5(CH_2)_2B(C_6F_5)_2$.

For Table of Contents Only